fluids

MDPI

Article

Comprehensive Perturbation Approach to Nonlinear Viscous Gravity–Capillary Surface Waves at Arbitrary Wavelengths in Finite Depth

Arash Ghahraman * and Gyula Bene

Department of Theoretical Physics, Institute of Physics, Eötvös Loránd University, Pázmány Péter sétány 1/A, 1117 Budapest, Hungary; bene.gyula@ttk.elte.hu

* Correspondence: ghahraman.arash@ttk.elte.hu

Abstract: This study presents a comprehensive analysis of the second-order perturbation theory applied to the Navier–Stokes equations governing free surface flows. We focus on gravity–capillary surface waves in incompressible viscous fluids of finite depth over a flat bottom. The amplitude of these waves is regarded as the perturbation parameter. A systematic derivation of a nonlinear-surface-wave equation is presented that fully takes into account dispersion, while nonlinearity is included in the leading order. However, the presence of infinitely many over-damped modes has been neglected and only the two least-damped modes are considered. The new surface-wave equation is formulated in wave-number space rather than real space and nonlinear terms contain convolutions making the equation an integro-differential equation. Some preliminary numerical results are compared with computational-modelling data obtained via open source CFD software OpenFOAM.

Keywords: shallow water; viscose fluid; surface waves; bifurcation analysis

PACS: 47.10.-g; 47.11.-j

Citation: Ghahraman, A.; Bene, G. Comprehensive Perturbation Approach to Nonlinear Viscous Gravity–Capillary Surface Waves at Arbitrary Wavelengths in Finite Depth. *Fluids* **2023**, *8*, 218. https://doi.org/10.3390/fluids8080218

Academic Editor: Jay Tang

Received: 21 June 2023
Revised: 19 July 2023
Accepted: 25 July 2023
Published: 27 July 2023

1. Introduction

A great number of studies have been conducted on gravity–capillary surface waves and there have been notable advancements in the study of nonlinear and dispersive gravity–capillary surface waves, with a particular focus on the effect of viscosity [1–11]. Several linear and weakly nonlinear equations have been suggested to represent the propagation of surface waves and dispersion relations [11–14]. The study of the nonlinear properties of capillary–gravity waves in infinitely deep water was initiated by Harrison [15] using a perturbation expansion. Harrison [15] focused on the influence of viscosity and surface tension. The author considered these parameters but did not provide an exact linear-dispersion relation. He found that the second approximations to both the velocity potential and the free-surface profile contained singularities for particular combinations of the reduced tension, gravity and wavelength.

As for the non-viscous case, the interested reader is referred to the excellent literature review article of Dias and Kharif [16]. Two-dimensional progressive gravity–capillary waves can also be studied at the interface between two fluids of different densities [17]. Hunt applied the Levi–Civita method for progressive and standing interface waves and obtained formulae of the wave profile and phase velocity up to the third order. In that paper, finite-depth fluid was studied. The author did not consider viscosity or surface tension and did not provide an exact linear-dispersion relation. Tsuji and Nagata [18] investigated the impact of surface tension in a scenario where deep and inviscid fluid was considered. They did not provide an exact linear-dispersion relation but contributed to the understanding of the role of surface tension in wave propagation, particularly in the absence of other parameters. They used a perturbation expansion in wave amplitude to the fifth order, for interfacial gravity waves of infinite depths. Their results suggested that the maximum value of the wave steepness may be limited by shear instability at the interface rather than the breaking condition at the interface. Matsuno [1,2] derived a Boussinesq-type model through an expansion in a steepness parameter $\epsilon = a/l$, where a represents the amplitude scale and l represents the wavelength scale. The author demonstrated that an appropriate extension of the integral kernel [19,20] establishes a connection with basic propagation models, such as the nonlinear Schrodinger equation (NLS) [21] and its variations (modified NLS—MNLS), with the most prominent being the Dysthe equation [22]. He pursued the perturbation analysis to the fourth order in wave steepness. One of the main effects at this order in infinite depth is precisely the influence of the wave-induced mean flow.

Viscosity serves as a pervasive damping mechanism [23,24], alongside other dissipation pathways such as impurities, obstacles and wave breaking. Its significance extends to the fundamental investigations of gravity waves [2,6,12,25]. More recently, a model for viscous deep-water waves was proposed by Dias, Dyachenko and Zakharov [26]. However, surface-tension effects have been neglected. The authors did not provide an exact linear-dispersion relation but their study enhanced the understanding of the influence of viscosity on nonlinear-wave behavior. In 2013, Liu, Hwung and Yang [27] considered the case of a two-fluid system with free surface. Second-order solutions were obtained, using the perturbation method. In cases of low viscosity, the vorticity is primarily concentrated within a narrow boundary layer in close proximity to the surface, as noted in previous studies [23,24,28,29]. Moreover, a multitude of authors have made significant contributions to comprehending the dispersion mechanism, wave propagation and stability analysis of capillary–gravity waves in finite depth [5,12,13,30–33].

In order to investigate the nonlinearities for surface water waves, Le Meur applied the Boussinesq approximation, which relates the amplitude (A), fluid depth (h) and wavelength (l)) as $A/h \propto h^2/l^2$. This condition together with the assumption of a large Reynolds number led to the separate treatment of the boundary layer from the bulk of the fluid [34]. Le Meur derived the exact dispersion relation in the linear regime, considering surface tension and viscosity effects in a viscous fluid of finite depth [33,34]. He concluded that for a large Reynolds number, $Re = \mathcal{O}((h/l)^{-5})$ represents the case of interest where viscous and gravitational effects balance.

The impact of viscosity on the nonlinear propagation of surface waves at the interface of air and a fluid of large depth is discussed in [35]. They proposed modified hydrodynamic boundary conditions to model both short and long waves. They showed that the linearity plays the main role in both gravity and capillary–gravity waves while the nonlinearity represents only small corrections. In the limit of infinite depth, authors utilized the exact linear-dispersion relation

$$(2 - i\frac{\omega}{\nu k^2})^2 + \frac{|k|(g + sk^2)}{\nu^2 k^4} = 4(1 - i\frac{\omega}{\nu k^2})^{\frac{1}{2}}\,, \tag{1}$$

where ν denotes the kinematic viscosity of the fluid and $s = \frac{\sigma}{\rho}$. σ stands for surface tension. Ghahraman and Bene [33] conducted an analysis of the linear dispersion relation in an unbounded channel with uniform depth, without imposing any constraints on the parameters. The authors focused on investigation of the conditions of wave propagation in the presence of viscosity and surface tension. It is discovered that both very short and very long waves are prohibited from propagating in thicker fluid layers, while the presence of two distinct length scales related to viscosity and surface tension is observed. Their findings indicate that there is a countably infinite number of modes present at any given horizontal wave number, but only those with the lowest damping rate are capable of describing propagating modes (see details in Section 3, after Equation (36)). All the other modes are over-damped. Further, in a fluid layer of sufficiently small thickness, there is a complete absence of wave propagation. Retaining the two modes with the least damping, a bidirectional evolution equation,

$$\frac{\partial^2\zeta}{\partial t^2} + i(\Omega^{(1)}(k) + \Omega^{(2)}(k))\frac{\partial\zeta}{\partial t} - \Omega^{(1)}(k)\Omega^{(2)}(k)\zeta = 0\,, \tag{2}$$

may be written down [33] for surface elevation $\zeta(k,t)$, where k denotes the horizontal wave number. It is a linear second-order differential equation at each wave number k and is applicable regardless of the feasibility of propagation. Note that $\Omega^{(1)}(k)$ and $\Omega^{(2)}(k)$ stand for the complex angular frequencies of the two modes.

Surface waves are typically nonlinear. When nonlinearity is factored in, it may stimulate previously dormant linear modes, potentially resulting in enhanced attenuation if the secondary modes are over-damped or, conversely, propagating the appearance if the primary modes are over-damped but the secondary modes are under-damped. Such impacts would not be anticipated under a linear approximation. Several intricate behaviors such as frequency modulation, wave mixing and mode generation, solitons, breeders, nonlinear resonances and modulational instabilities may emerge due to nonlinearity in wave equations, predominantly in non-dissipative cases. It is expected that these phenomena persist in some form even when dissipation is present, thereby driving the need for an effective tool to scrutinize these effects.

It is intriguing what the interplay is between dispersion, dissipation and nonlinearity. For instance, by considering the simplified nonlinear-wave equation

$$\frac{\partial\zeta}{\partial t} + \frac{\partial\zeta}{\partial x} + \frac{\partial^2\zeta}{\partial x^2} + \frac{\partial^3\zeta}{\partial x^3} + \frac{1}{2}\zeta\frac{\partial\zeta}{\partial x} = 0,$$

it is well known what happens if one or more of these factors are absent. When the second derivative (representing dissipation) is removed, the Korteweg–de Vries (KdV) equation, a well-established solitonic solution, arises. A scenario without the third derivative term (denoting dispersion) leads to an equation where dissipation instigates concurrent decay and wave-profile broadening, with nonlinearity engendering asymmetry in the wave profile. Nevertheless, the picture becomes less discernible when all three aspects are in operation. Moreover, it is also a question what the correct nonlinear-wave equation is for capillary–gravity waves. Extant literature largely relies on approximations such as the Boussinesq approximation. This research aims to present a tool by introducing a method that incorporates nonlinear terms to a leading order without depending on such approximations.

This paper aims to generalize the results of [33], especially Equation (2), by including the leading nonlinear terms in the Navier–Stokes equation, as well as boundary conditions. In order to achieve this objective, we employ a perturbative approach to solve the Navier–Stokes equations for the surface-wave problem up to the second order, where the wave amplitude is considered to be a small parameter. This method allows for the systematic study of nonlinearity in various fluid phenomena [36–43]. At this stage, the calculation is still completely general; in particular, all the modes are included. Then, we look for a generalization of Equation (2). We write down the most general quadratic second-order differential equation that is allowed via horizontal translational symmetry. We solve this equation perturbatively to the second order and then compare the result with that of the previous perturbation theory of surface waves, where we keep only the two least-damped modes. This comparison results in a well-defined nonlinear integro-differential equation for surface elevations that is self-consistent. Incorporating further modes would lead to the emergence of time derivatives of a higher order than two, a feature that is also observed at the linear level. Table 1 presents a summary and comparison of the existing literature with regards to their parameters, dispersion relations and the methodologies employed. Based on the findings presented in Table 1, only the works conducted by Le Meur [34] and Ghahraman and Bene [33] derive an exact linear-dispersion relation for finite fluid depth in the presence of viscosity, gravity and surface tension. In contrast, the present study explores nonlinearity without resorting to any further approximation or restriction than the smallness of the wave amplitude, distinguishing it from Le Meur's methodology.

The plan of the paper is as follows. In Section 2, a formulation of the problem is given. First-order and second-order approximations are discussed in Sections 3 and 4, respectively. In Section 5, we derive the surface-wave equation based on perturbation theory. The results are summarized and discussed in the concluding section, Section 6. Some longer expressions are relegated to the Appendix A.

Table 1. Comparing literature studies by physical parameters.

Authors	Finite Depth	Viscosity	Surface Tension	Exact Dispersion Relation	Method
Harrison [15]	X	✓	✓	X	Perturbation expansion
Dias and Kharif [16]	X	X	X	✓	–
Hunt [17]	✓	X	X	X	Levi–Civita's method
Tsuji and Nagata [18]	X	X	✓	X	Perturbation expansion
Matsuno [1]	✓	X	X	X	Principles of complex functions and a methodical perturbation theory
Dysthe [22]	X	X	X	X	Perturbation expansion
Dias, Dyachenko and Zakharov [26]	X	✓	X	X	Helmholtz decomposition
Le Meur [34]	✓	✓	✓	✓	Boussinesq approximation
Armaroli [35]	X	✓	✓	✓	–
Ghahraman and Bene [33]	✓	✓	✓	✓	Linear approximation

2. Formulation of the Problem

Consider the irrotational flow of an incompressible inviscid fluid with a free surface. A Cartesian coordinate system is adopted, with the x-axis located on the still-water plane and with the z-axis pointing vertically upwards. The fluid domain is bounded by the bed at $z = -h$ and the free surface at $z = \zeta(x,t)$ (Figure 1). The Navier–Stokes (NS) equations in the bulk are:

$$\frac{\partial \boldsymbol{V}}{\partial t} + (\boldsymbol{V} \cdot \nabla)\boldsymbol{V} - \nu \triangle \boldsymbol{V} = \nabla(-\frac{p}{\rho} - gz) \tag{3}$$

Since the right-hand side is a full gradient, we have

$$\frac{\partial}{\partial z}\left(\frac{\partial u}{\partial t} + u\frac{\partial u}{\partial x} + w\frac{\partial u}{\partial z} - \nu \triangle u\right) = \frac{\partial}{\partial x}\left(\frac{\partial w}{\partial t} + u\frac{\partial w}{\partial x} + w\frac{\partial w}{\partial z} - \nu \triangle w\right) \tag{4}$$

with bottom boundary conditions

$$u(z=-h) = w(z=-h) = 0 \tag{5}$$

and horizontal and vertical components of net force at the surface (up to second-order precision in amplitudes):

$$\begin{aligned}\rho\nu\left(\frac{\partial u}{\partial z} + \frac{\partial w}{\partial x}\right) &= \frac{\partial \zeta}{\partial x}\left(p_0 - p + 2\rho\nu\frac{\partial u}{\partial x} - \sigma\frac{\partial^2 \zeta}{\partial x^2}\right) \\ &\quad - \zeta\frac{\partial}{\partial z}\left[\rho\nu\left(\frac{\partial u}{\partial z} + \frac{\partial w}{\partial x}\right) - \frac{\partial \zeta}{\partial x}(p_0 - p)\right]\end{aligned} \tag{6}$$

$$p_0 - p + 2\rho\nu\frac{\partial w}{\partial z} - \sigma\frac{\partial^2 \zeta}{\partial x^2} = -\zeta\frac{\partial}{\partial z}\left(p_0 - p + 2\rho\nu\frac{\partial w}{\partial z}\right) + \frac{\partial \zeta}{\partial x}\rho\nu\left(\frac{\partial u}{\partial z} + \frac{\partial w}{\partial x}\right). \tag{7}$$

Further, we have the kinematic condition for the surface

$$\frac{\partial \zeta}{\partial t} - w = -u\frac{\partial \zeta}{\partial x} + \zeta\frac{\partial w}{\partial z}\,. \tag{8}$$

By eliminating the pressure from Equations (6) and (7) with the help of the Navier–Stokes equations, we have the following equations, respectively.

$$\frac{\partial u}{\partial z} + \frac{\partial w}{\partial x} + \zeta\frac{\partial}{\partial z}\left(\frac{\partial u}{\partial z} + \frac{\partial w}{\partial x}\right) = 0 \tag{9}$$

$$\begin{aligned}\frac{\partial u}{\partial t} + u\frac{\partial u}{\partial x} + w\frac{\partial u}{\partial z} - \nu\triangle u + 2\nu\frac{\partial^2 w}{\partial x\partial z} - \frac{\sigma}{\rho}\frac{\partial^3 \zeta}{\partial x^3} = -\zeta\left(\frac{\partial^2 w}{\partial t\partial x} - \nu\frac{\partial^3 w}{\partial x^3} + \nu\frac{\partial^3 w}{\partial x\partial z^2}\right)\\ - \frac{\partial \zeta}{\partial x}\left(g + \frac{\partial w}{\partial t} - 2\nu\frac{\partial^2 w}{\partial x^2} + \nu\frac{\partial^2 w}{\partial z^2} - \nu\frac{\partial^2 u}{\partial x\partial z}\right) + \nu\frac{\partial^2 \zeta}{\partial x^2}\left(\frac{\partial u}{\partial z} + \frac{\partial w}{\partial x}\right)\end{aligned} \tag{10}$$

As a result, the main equations in this study are Equations (4), (5) and (8)–(10).

Assuming incompressible fluid, we may express the velocity components in terms of the stream function as

$$u = -\frac{\partial \psi}{\partial z} \tag{11}$$

$$w = \frac{\partial \psi}{\partial x} \tag{12}$$

Inserting Equations (11) and (12) into the previous equations, we obtain

$$\frac{\partial \triangle\psi}{\partial t} - \nu\triangle\triangle\psi = \frac{\partial \psi}{\partial x}\frac{\partial \triangle\psi}{\partial z} - \frac{\partial \psi}{\partial z}\frac{\partial \triangle\psi}{\partial x} \tag{13}$$

in the bulk and

$$\frac{\partial \psi}{\partial x} = 0 \tag{14}$$

$$\frac{\partial \psi}{\partial z} = 0 \tag{15}$$

at the bottom ($z = -h$). The surface boundary conditions are (at $z = 0$):

$$\frac{\partial \zeta}{\partial t} - \frac{\partial \psi}{\partial x} = \frac{\partial \psi}{\partial z}\frac{\partial \zeta}{\partial x} + \zeta\frac{\partial^2 \psi}{\partial x\partial z}\,, \tag{16}$$

$$\frac{\partial^2 \psi}{\partial x^2} - \frac{\partial^2 \psi}{\partial z^2} + \zeta\frac{\partial^3 \psi}{\partial x^2\partial z} - \zeta\frac{\partial^3 \psi}{\partial z^3} = 0 \tag{17}$$

and

$$\begin{aligned}-\frac{\partial^2 \psi}{\partial t\partial z} + 3\nu\frac{\partial^2 \psi}{\partial x^2\partial z} + \nu\frac{\partial^2 \psi}{\partial z^3} + g\frac{\partial \zeta}{\partial x} - \frac{\sigma}{\rho}\frac{\partial^3 \zeta}{\partial x^3} = \frac{\partial \psi}{\partial x}\frac{\partial^2 \psi}{\partial z^2} - \frac{\partial \psi}{\partial z}\frac{\partial^2 \psi}{\partial x\partial z}\\ + \zeta\left[-\frac{\partial^3 \psi}{\partial t\partial x^2} + \nu\left(\frac{\partial^4 \psi}{\partial x^4} - \frac{\partial^4 \psi}{\partial x^2\partial z^2}\right)\right] + \frac{\partial \zeta}{\partial x}\left[-\frac{\partial^2 \psi}{\partial t\partial x} + 2\nu\left(\frac{\partial^3 \psi}{\partial x^3} - \frac{\partial^3 \psi}{\partial x\partial z^2}\right)\right]\\ + \nu\frac{\partial^2 \zeta}{\partial x^2}\left(\frac{\partial^2 \psi}{\partial x^2} - \frac{\partial^2 \psi}{\partial z^2}\right).\end{aligned} \tag{18}$$

We are looking for a solution in a form

$$\psi = \psi^{[1]} + \psi^{[2]}\,, \tag{19}$$

$$\zeta = \zeta^{[1]} + \zeta^{[2]}\,, \tag{20}$$

where the superscript refers to the order.

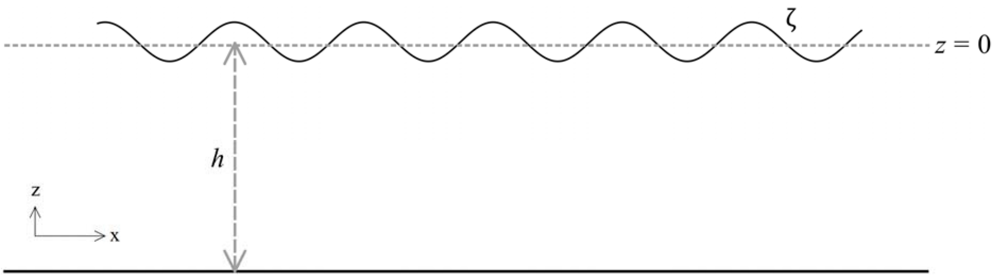

Figure 1. Schematic description of the surface waves over flat bottom. The graph of time-dependent free surface is given by $z = \zeta(x,t)$.

3. First-Order Solutions

Inserting decompositions (19) and (20) into the equations, we have in the first order

$$\frac{\partial \triangle \psi^{[1]}}{\partial t} - \nu \triangle\triangle \psi^{[1]} = 0 \tag{21}$$

in the bulk ($-h \le z \le 0$),

$$\frac{\partial \psi^{[1]}}{\partial x} = 0 \tag{22}$$

$$\frac{\partial \psi^{[1]}}{\partial z} = 0 \tag{23}$$

at the bottom ($z = -h$) and

$$\frac{\partial \zeta^{[1]}}{\partial t} - \frac{\partial \psi^{[1]}}{\partial x} = 0\,, \tag{24}$$

$$\frac{\partial^2 \psi^{[1]}}{\partial x^2} - \frac{\partial^2 \psi^{[1]}}{\partial z^2} = 0\,, \tag{25}$$

$$-\frac{\partial^2 \psi^{[1]}}{\partial t \partial z} + 3\nu \frac{\partial^2 \psi^{[1]}}{\partial x^2 \partial z} + \nu \frac{\partial^2 \psi^{[1]}}{\partial z^3} + g\frac{\partial \zeta^{[1]}}{\partial x} - \frac{\sigma}{\rho}\frac{\partial^3 \zeta^{[1]}}{\partial x^3} = 0 \tag{26}$$

on the surface ($z = 0$).

Generally, the first-order solution is an integral over wave number k.

$$\psi^{[1]} = \sum_j \int_{-\infty}^{\infty} dk\, C^{(j)}(k) F^{(j)}(k,z) \exp(i\varphi^{(j)}) + c.c. \tag{27}$$

$$\zeta^{[1]} = -\sum_j \int_{-\infty}^{\infty} dk\, C^{(j)}(k) \frac{k}{\Omega^{(j)}} F^{(j)}(k,0) \exp(i\varphi^{(j)}) + c.c. \tag{28}$$

where $\varphi^{(j)} = kx - \Omega^{(j)} t$ and

$$\begin{aligned} F^{(j)}(k,z) &= A^{(j)} \cosh k(z+h) - A^{(j)} \cosh \kappa^{(j)}(z+h) \\ &\quad + B^{(j)} \sinh \kappa^{(j)}(z+h) - \frac{\kappa^{(j)}}{k} B^{(j)} \sinh k(z+h) \end{aligned} \tag{29}$$

$$\begin{aligned} A^{(j)} &= 2\kappa^{(j)} k \sinh(kh) - \left(\kappa^{(j)2} + k^2\right) \sinh(\kappa^{(j)} h) \\ B^{(j)} &= 2k^2 \cosh(kh) - \left(\kappa^{(j)2} + k^2\right) \cosh(\kappa^{(j)} h) \,. \end{aligned} \tag{30}$$

The angular frequency reads

$$\Omega^{(j)} = i\nu\left(\kappa^{(j)2} - k^2\right) . \tag{31}$$

Modes are labelled by horizontal wave number k (a continuous parameter) and discrete $\kappa^{(j)}$ values which are solutions of the following equation [33,44]

$$\begin{aligned} & K(Q \sinh K \cosh Q - K \cosh K \sinh Q)(1 + sK^2) \\ & + p\Big[-4K^2 Q\left(K^2 + Q^2\right) + Q\left(Q^4 + 2K^2Q^2 + 5K^4\right) \cosh K \cosh Q \\ & - K\left(Q^4 + 6K^2Q^2 + K^4\right) \sinh K \sinh Q\Big] = 0 \,. \end{aligned} \tag{32}$$

Here

$$K = kh \,, \tag{33}$$

$$Q = \kappa h \,, \tag{34}$$

$$p = \frac{\nu^2}{gh^3} \,, \tag{35}$$

$$s = \frac{\sigma}{\rho g h^2} \,. \tag{36}$$

Note that Equation (32) simplifies to Equation (1) in the deep fluid limit $h \to \infty$.

Figure 2 demonstrates that a large number of solutions to Equation (32) are achieved by setting constant parameters and generating branches that alter as K changes. The imaginary parts of the frequencies are displayed. Nonzero real parts appear when two branches merge [33]. Only the lowest two branches are displayed in Figure 3, both the real and imaginary parts of the frequencies. At this parameter setting, there is a broader range of wave numbers where propagation of waves is possible.

Summation in (27) and (28) is understood over the possible branches (denoted by bracketed upper indices) of the dispersion relation $\Omega(k)$. Note that if κ is a solution, so is κ^* at the same k value, though it may yield a different Ω branch. The branches of the dispersion relation at k are the same as at $-k$. This allows indexing in the following way:

$$\begin{aligned} \kappa^{(j)}(-k) &= \kappa^{(j)*}(k) \\ \Omega^{(j)}(-k) &= -\Omega^{(j)*}(k) \,. \end{aligned} \tag{37}$$

Thus, we have

$$\psi^{[1]} = \sum_j \int_{-\infty}^{\infty} dk \exp(ikx) F^{(j)}(k,z) \times \left[C^{(j)}(k) + C^{(j)*}(-k)\right] \exp(-i\Omega^{(j)}(k)t) \tag{38}$$

$$\zeta^{[1]} = -\sum_j \int_{-\infty}^{\infty} dk \exp(ikx) \frac{k}{\Omega^{(j)}} F^{(j)}(k,0) \times \left[C^{(j)}(k) + C^{(j)*}(-k)\right] \exp(-i\Omega^{(j)}(k)t) \tag{39}$$

Since the coefficients $C^{(j)}(k)$ always appear in the combination $C^{(j)}(k) + C^{(j)*}(-k)$, henceforth we shall denote this sum with $C^{(j)}(k)$, satisfying $C^{(j)}(-k) = C^{(j)*}(k)$. Note that

$C^{(j)}(k)$ may be expressed in terms of the spatial Fourier transform of the initial conditions $\zeta^{[1]}(t)$ and $\dot{\zeta}^{[1]}(t)$, if we keep just two branches of the dispersion relation.

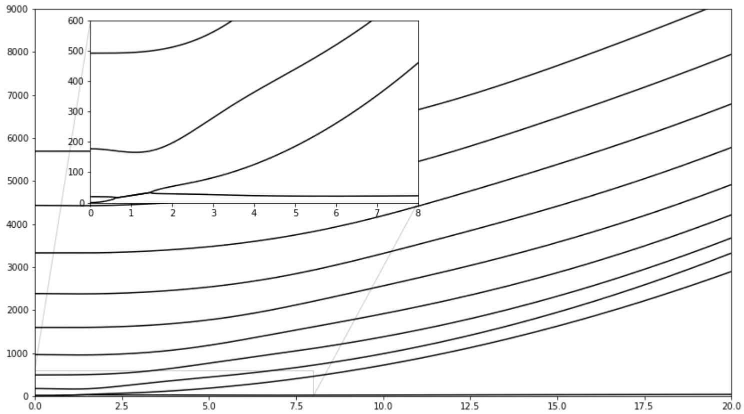

Figure 2. For glycerin at $p = 0.077$, the first 10 branches of imaginary parts of frequencies are illustrated. When K increases, the two lowest branches meet and give rise to a nonzero real part, but the majority of frequencies remain totally imaginary.

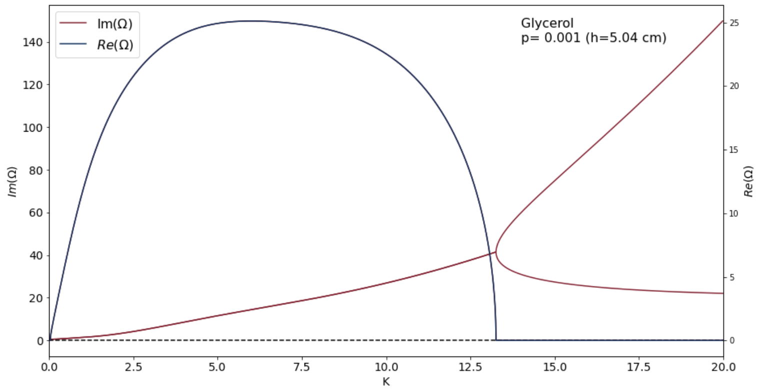

Figure 3. The real and imaginary parts of frequencies corresponding to the lowest-lying branches versus K for glycerin at $p = 0.001$ ($h = 5.04$ cm).

4. Second-Order Solutions

In second-order approximation, the main system of equations are

$$\frac{\partial \triangle \psi^{[2]}}{\partial t} - \nu \triangle \triangle \psi^{[2]} = \frac{\partial \psi^{[1]}}{\partial x} \frac{\partial \triangle \psi^{[1]}}{\partial z} - \frac{\partial \psi^{[1]}}{\partial z} \frac{\partial \triangle \psi^{[1]}}{\partial x} \tag{40}$$

in the bulk and

$$\frac{\partial \psi^{[2]}}{\partial x} = 0 \tag{41}$$

$$\frac{\partial \psi^{[2]}}{\partial z} = 0 \tag{42}$$

at the bottom ($z = -h$). The surface boundary conditions are (at $z = 0$):

$$\frac{\partial \zeta^{[2]}}{\partial t} - \frac{\partial \psi^{[2]}}{\partial x} = \frac{\partial \psi^{[1]}}{\partial z} \frac{\partial \zeta^{[1]}}{\partial x} + \zeta^{[1]} \frac{\partial^2 \psi^{[1]}}{\partial x \partial z}\ , \tag{43}$$

$$\frac{\partial^2 \psi^{[2]}}{\partial x^2} - \frac{\partial^2 \psi^{[2]}}{\partial z^2} = -\zeta^{[1]} \left(\frac{\partial^3 \psi^{[1]}}{\partial x^2 \partial z} - \frac{\partial^3 \psi^{[1]}}{\partial z^3} \right) \tag{44}$$

and

$$
\begin{aligned}
&-\frac{\partial^2\psi^{[2]}}{\partial t\partial z}+3\nu\frac{\partial^3\psi^{[2]}}{\partial x^2\partial z}+\nu\frac{\partial^3\psi^{[2]}}{\partial z^3}+g\frac{\partial\zeta^{[2]}}{\partial x}-\frac{\sigma}{\rho}\frac{\partial^3\zeta^{[2]}}{\partial x^3}=\frac{\partial\psi^{[1]}}{\partial x}\frac{\partial^2\psi^{[1]}}{\partial z^2}\\
&-\frac{\partial\psi^{[1]}}{\partial z}\frac{\partial^2\psi^{[1]}}{\partial x\partial z}+\zeta^{[1]}\left[-\frac{\partial^3\psi^{[1]}}{\partial t\partial x^2}+\nu\left(\frac{\partial^4\psi^{[1]}}{\partial x^4}-\frac{\partial^4\psi^{[1]}}{\partial x^2\partial z^2}\right)\right]\\
&+\frac{\partial\zeta^{[1]}}{\partial x}\left[-\frac{\partial^2\psi^{[1]}}{\partial t\partial x}+2\nu\left(\frac{\partial^3\psi^{[1]}}{\partial x^3}-\frac{\partial^3\psi^{[1]}}{\partial x\partial z^2}\right)\right]\\
&+\nu\frac{\partial^2\zeta^{[1]}}{\partial x^2}\left(\frac{\partial^2\psi^{[1]}}{\partial x^2}-\frac{\partial^2\psi^{[1]}}{\partial z^2}\right)
\end{aligned}
\tag{45}
$$

The second-order calculation requires evaluation of the right-hand side of Equation (40), which is quadratic in $\psi^{[1]}$; therefore, one obtains a double integral. Explicitly, we obtain for the right-hand side of Equation (40)

$$
\begin{aligned}
&\sum_a\sum_b\int_{-\infty}^{\infty}dk_1\int_{-\infty}^{\infty}dk_2\,C_1^{(a)}C_2^{(b)}\exp\left\{i(k_1+k_2)x-i\left[\Omega_1^{(a)}+\Omega_2^{(b)}\right]t\right\}\\
&\times\Big\{\bar\alpha_{c+}^{(ab)}\cosh[(k_1+k_2)(z+h)]+\bar\beta_{c+}^{(ab)}\cosh\left[(\kappa_1^{(a)}+k_2)(z+h)\right]\\
&\quad+\bar\gamma_{c+}^{(ab)}\cosh\left[(k_1+\kappa_2^{(b)})(z+h)\right]+\bar\delta_{c+}^{(ab)}\cosh\left[(\kappa_1^{(a)}+\kappa_2^{(b)})(z+h)\right]\\
&\quad+\bar\alpha_{c-}^{(ab)}\cosh[(k_1-k_2)(z+h)]+\bar\beta_{c-}^{(ab)}\cosh\left[(\kappa_1^{(a)}-k_2)(z+h)\right]\\
&\quad+\bar\gamma_{c-}^{(ab)}\cosh\left[(k_1-\kappa_2^{(b)})(z+h)\right]+\bar\delta_{c-}^{(ab)}\cosh\left[(\kappa_1^{(a)}-\kappa_2^{(b)})(z+h)\right]\\
&\quad+\bar\alpha_{s+}^{(ab)}\sinh[(k_1+k_2)(z+h)]+\bar\beta_{s+}^{(ab)}\sinh\left[(\kappa_1^{(a)}+k_2)(z+h)\right]\\
&\quad+\bar\gamma_{s+}^{(ab)}\sinh\left[(k_1+\kappa_2^{(b)})(z+h)\right]+\bar\delta_{s+}^{(ab)}\sinh\left[(\kappa_1^{(a)}+\kappa_2^{(b)})(z+h)\right]\\
&\quad+\bar\alpha_{s-}^{(ab)}\sinh[(k_1-k_2)(z+h)]+\bar\beta_{s-}^{(ab)}\sinh\left[(\kappa_1^{(a)}-k_2)(z+h)\right]\\
&\quad+\bar\gamma_{s-}^{(ab)}\sinh\left[(k_1-\kappa_2^{(b)})(z+h)\right]+\bar\delta_{s-}^{(ab)}\sinh\left[(\kappa_1^{(a)}-\kappa_2^{(b)})(z+h)\right]\Big\}\,.
\end{aligned}
\tag{46}
$$

Note that $\bar\alpha_{c\pm}^{(ab)}=\bar\alpha_{s\pm}^{(ab)}=0$. Other coefficients depend on both k_1 and k_2 (see Appendix A). The solution of (40) can be written in a similar form:

$$
\begin{aligned}
\psi^{[2]} &= \sum_a \sum_b \int_{-\infty}^{\infty} dk_1 \int_{-\infty}^{\infty} dk_2\, C_1^{(a)} C_2^{(b)} \exp\left\{ i(k_1+k_2)x - i\left[\Omega_1^{(a)} + \Omega_2^{(b)}\right] t \right\} \\
&\times \Big\{ \alpha_{c+}^{(ab)} \cosh[(k_1+k_2)(z+h)] + \beta_{c+}^{(ab)} \cosh\left[(\kappa_1^{(a)}+k_2)(z+h)\right] \\
&+ \gamma_{c+}^{(ab)} \cosh\left[(k_1+\kappa_2^{(b)})(z+h)\right] + \delta_{c+}^{(ab)} \cosh\left[(\kappa_1^{(a)}+\kappa_2^{(b)})(z+h)\right] \\
&+ \alpha_{c-}^{(ab)} \cosh[(k_1-k_2)(z+h)] + \beta_{c-}^{(ab)} \cosh\left[(\kappa_1^{(a)}-k_2)(z+h)\right] \\
&+ \gamma_{c-}^{(ab)} \cosh\left[(k_1-\kappa_2^{(b)})(z+h)\right] + \delta_{c-}^{(ab)} \cosh\left[(\kappa_1^{(a)}-\kappa_2^{(b)})(z+h)\right] \\
&+ \alpha_{s+}^{(ab)} \sinh[(k_1+k_2)(z+h)] + \beta_{s+}^{(ab)} \sinh\left[(\kappa_1^{(a)}+k_2)(z+h)\right] \\
&+ \gamma_{s+}^{(ab)} \sinh\left[(k_1+\kappa_2^{(b)})(z+h)\right] + \delta_{s+}^{(ab)} \sinh\left[(\kappa_1^{(a)}+\kappa_2^{(b)})(z+h)\right] \\
&+ \alpha_{s-}^{(ab)} \sinh[(k_1-k_2)(z+h)] + \beta_{s-}^{(ab)} \sinh\left[(\kappa_1^{(a)}-k_2)(z+h)\right] \\
&+ \gamma_{s-}^{(ab)} \sinh\left[(k_1-\kappa_2^{(b)})(z+h)\right] + \delta_{s-}^{(ab)} \sinh\left[(\kappa_1^{(a)}-\kappa_2^{(b)})(z+h)\right] \Big\} + \psi_h^{[2]} \,. \qquad (47)
\end{aligned}
$$

Here again $\alpha_{c\pm}^{(ab)} = \alpha_{s\pm}^{(ab)} = 0$. Other coefficients can be calculated directly from Equation (40) (see Appendix A). The homogeneous part $\psi_h^{[2]}$ is written as

$$
\begin{aligned}
\psi_h^{[2]} &= \sum_a \sum_b \int_{-\infty}^{\infty} dk_1 \int_{-\infty}^{\infty} dk_2\, \exp\left\{ i(k_1+k_2)x - i\left[\Omega_1^{(a)} + \Omega_2^{(b)}\right] t \right\} \\
&\times \Big\{ \epsilon_c^{(ab)} \cosh[(k_1+k_2)(z+h)] + \epsilon_s^{(ab)} \sinh[(k_1+k_2)(z+h)] \\
&+ \mu_c^{(ab)} \cosh\left[q_{12}^{(ab)}(z+h)\right] + \mu_s^{(ab)} \sinh\left[q_{12}^{(ab)}(z+h)\right] \Big\} \,, \qquad (48)
\end{aligned}
$$

where

$$
q_{12}^{(ab)2} = \kappa_1^{(a)2} + \kappa_2^{(b)2} + 2k_1k_2 \,. \qquad (49)
$$

Coefficients $\epsilon_c^{(ab)}$, $\epsilon_s^{(ab)}$, $\mu_c^{(ab)}$, $\mu_s^{(ab)}$ are to be determined from boundary conditions (41)–(45). Bottom boundary conditions (41) and (42) yield the equations

$$
\epsilon_c^{(ab)} + \mu_c^{(ab)} = -\alpha_{c+}^{(ab)} - \beta_{c+}^{(ab)} - \gamma_{c+}^{(ab)} - \delta_{c+}^{(ab)} - \alpha_{c-}^{(ab)} - \beta_{c-}^{(ab)} - \gamma_{c-}^{(ab)} - \delta_{c-}^{(ab)} \qquad (50)
$$

and

$$
\begin{aligned}
(k_1+k_2)\epsilon_s^{(ab)} + q_{12}^{(ab)} \mu_s^{(ab)} = &- (k_1+k_2)\alpha_{s+}^{(ab)} - (\kappa_1^{(a)}+k_2)\beta_{s+}^{(ab)} \\
&- (k_1+\kappa_2^{(b)})\gamma_{s+}^{(ab)} - (\kappa_1^{(a)}+\kappa_2^{(b)})\delta_{s+}^{(ab)} \\
&- (k_1-k_2)\alpha_{s-}^{(ab)} - (\kappa_1^{(a)}-k_2)\beta_{s-}^{(ab)} \\
&- (k_1-\kappa_2^{(b)})\gamma_{s-}^{(ab)} - (\kappa_1^{(a)}-\kappa_2^{(b)})\delta_{s-}^{(ab)} \qquad (51)
\end{aligned}
$$

respectively. Surface boundary condition (43) determines $\zeta^{[2]}$ as

$$
\begin{aligned}
\zeta^{[2]} = \sum_a \sum_b \int_{-\infty}^{\infty} dk_1 \int_{-\infty}^{\infty} dk_2 \, C_1^{(a)} C_2^{(b)} \; \exp\left\{ i(k_1+k_2)x - i\left[\Omega_1^{(a)} + \Omega_2^{(b)}\right] t \right\} \\
\times \left\{ s^{(ab)} - \frac{k_1+k_2}{\Omega_1^{(a)} + \Omega_2^{(b)}} \left(\cosh[(k_1+k_2)h]\epsilon_c^{(ab)} + \sinh[(k_1+k_2)h]\epsilon_s^{(ab)} \right.\right. \\
\left.\left. + \cosh\left[q_{12}^{(ab)} h\right] \mu_c^{(ab)} + \sinh\left[q_{12}^{(ab)} h\right] \mu_s^{(ab)} \right) \right\}
\end{aligned} \tag{52}
$$

Here, $s^{(ab)}$ is a function of both k_1 and k_2; its explicit expression is lengthy and is given therefore as a Appendix A item. Equations (44) and (45) combined with Equations (50)–(52) provide us with the relations

$$
\begin{aligned}
& \left\{ \left(\kappa_1^{(a)2} + \kappa_2^{(b)2} + k_1^2 + k_2^2 + 4k_1k_2 \right) \cosh\left(q_{12}^{(ab)} \right) - 2(k_1+k_2)^2 \cosh(k_1+k_2) \right\} \mu_c^{ab} \\
+ & \left\{ \left(\kappa_1^{(a)2} + \kappa_2^{(b)2} + k_1^2 + k_2^2 + 4k_1k_2 \right) \sinh\left(q_{12}^{(ab)} \right) - 2(k_1+k_2)^2 \sinh(k_1+k_2) \right\} \mu_s^{(ab)} \\
= & \; r^{(ab)}
\end{aligned} \tag{53}
$$

and

$$
\begin{aligned}
& \left\{ 2q_{12}^{(ab)} (k_1+k_2)^2 \sinh\left(q_{12}^{(ab)} \right) - (k_1+k_2) \left(\kappa_1^{(a)2} + \kappa_2^{(b)2} + k_1^2 + k_2^2 + 4k_1k_2 \right) \sinh(k_1+k_2) \right. \\
& \left. + \frac{(k_1+k_2)^2 \left(1 + s(k_1+k_2)^2 \right)}{p\left[k_1^2 + k_2^2 - \kappa_1^{(a)2} - \kappa_2^{(b)2} \right]} \left[\cosh(k_1+k_2) - \cosh\left(q_{12}^{(ab)} \right) \right] \right\} \mu_c^{(ab)} \\
& + \left\{ 2q_{12}^{(ab)} (k_1+k_2)^2 \cosh\left(q_{12}^{(ab)} \right) - q_{12}^{(ab)} \left(\kappa_1^{(a)2} + \kappa_2^{(b)2} + k_1^2 + k_2^2 + 4k_1k_2 \right) \cosh(k_1+k_2) \right. \\
& \left. + \frac{(k_1+k_2) \left(1 + s(k_1+k_2)^2 \right)}{p\left[k_1^2 + k_2^2 - \kappa_1^{(a)2} - \kappa_2^{(b)2} \right]} \left[q_{12}^{(ab)} \sinh(k_1+k_2) - (k_1+k_2) \sinh\left(q_{12}^{(ab)} \right) \right] \right\} \mu_s^{(ab)} \\
& = t^{(ab)}
\end{aligned} \tag{54}
$$

respectively. The right-hand sides $r^{(ab)}$, $t^{(ab)}$ no longer contain any unknowns; they are well-determined functions of k_1 and k_2. Their explicit expressions are again given as a Appendix A item.

Solving Equations (50), (51), (53) and (54) we obtain finally

$$
\zeta^{[2]} = \sum_a \sum_b \int_{-\infty}^{\infty} dk_1 \int_{-\infty}^{\infty} dk_2 \, C_1^{(a)} C_2^{(b)} \; S^{(ab)}(k_1,k_2) \exp\left\{ i(k_1+k_2)x - i\left[\Omega_1^{(a)} + \Omega_2^{(b)} \right] t \right\}, \tag{55}
$$

where $S^{(ab)}(k_1,k_2)$ stands for the second line of Equation (52).

5. Surface-Wave Equation

Equations (28) and (55) yield the solution for the surface shape up to the second order. We discuss now whether and how one can derive a single wave equation for the surface shape to this order, without reference to the underlying bulk Navier–Stokes equations. Provided that we keep only a single pair of Ω values of the dispersion relation, this equation—due to translation symmetry—in k-space must have the form

$$
\begin{aligned}
&\frac{\partial^2\tilde{\zeta}(k)}{\partial t^2} + i\Big[\Omega^{(1)}(k) + \Omega^{(2)}(k)\Big]\frac{\partial\tilde{\zeta}(k)}{\partial t} - \Omega^{(1)}(k)\Omega^{(2)}(k)\tilde{\zeta}(k) \\
&+ \int_{-\infty}^{\infty} dk'\ \tilde{W}_1(k',k-k')\tilde{\zeta}(k')\tilde{\zeta}(k-k') \\
&+\frac{1}{2}\int_{-\infty}^{\infty} dk'\ \tilde{W}_2(k',k-k')\left(\tilde{\zeta}(k')\frac{\partial\tilde{\zeta}(k-k')}{\partial t} + \frac{\partial\tilde{\zeta}(k')}{\partial t}\tilde{\zeta}(k-k')\right) \\
&+\frac{1}{2}\int_{-\infty}^{\infty} dk'\ \tilde{W}_3(k',k-k')\left(\tilde{\zeta}(k')\frac{\partial\tilde{\zeta}(k-k')}{\partial t} - \frac{\partial\tilde{\zeta}(k')}{\partial t}\tilde{\zeta}(k-k')\right) \\
&+ \int_{-\infty}^{\infty} dk'\ \tilde{W}_4(k',k-k')\frac{\partial\tilde{\zeta}(k')}{\partial t}\frac{\partial\tilde{\zeta}(k-k')}{\partial t} = 0\,,
\end{aligned} \tag{56}
$$

where functions $\tilde{W}_1(k_1,k_2)$, $\tilde{W}_2(k_1,k_2)$ and $\tilde{W}_4(k_1,k_2)$ are symmetric, while $\tilde{W}_3(k_1,k_2)$ is antisymmetric with respect to the exchange of their variables:

$$
\begin{aligned}
\tilde{W}_1(k_1,k_2) &= \tilde{W}_1(k_2,k_1) \\
\tilde{W}_2(k_1,k_2) &= \tilde{W}_2(k_2,k_1) \\
\tilde{W}_4(k_1,k_2) &= \tilde{W}_4(k_2,k_1) \\
\tilde{W}_3(k_1,k_2) &= -\tilde{W}_3(k_2,k_1)\,.
\end{aligned} \tag{57}
$$

Alternatively, one may write

$$
\begin{aligned}
&\frac{\partial^2\tilde{\zeta}(k)}{\partial t^2} + i\Big[\Omega^{(1)}(k) + \Omega^{(2)}(k)\Big]\frac{\partial\tilde{\zeta}(k)}{\partial t} - \Omega^{(1)}(k)\Omega^{(2)}(k)\tilde{\zeta}(k) \\
&+ \int_{-\infty}^{\infty} dk'\ \tilde{W}_{--}(k',k-k')\tilde{\zeta}(k')\tilde{\zeta}(k-k') \\
&+2\int_{-\infty}^{\infty} dk'\ \tilde{W}_{-+}(k',k-k')\tilde{\zeta}(k')\frac{\partial\tilde{\zeta}(k-k')}{\partial t} \\
&+ \int_{-\infty}^{\infty} dk'\ \tilde{W}_{++}(k',k-k')\frac{\partial\tilde{\zeta}(k')}{\partial t}\frac{\partial\tilde{\zeta}(k-k')}{\partial t} = 0
\end{aligned} \tag{58}
$$

where

$$
\begin{aligned}
\tilde{W}_{--}(k_1,k_2) &= \tilde{W}_1(k_1,k_2)\,, \\
\tilde{W}_{-+}(k_1,k_2) &= \frac{1}{2}\big(\tilde{W}_2(k_1,k_2) + \tilde{W}_3(k_1,k_2)\big)\,, \\
\tilde{W}_{+-}(k_1,k_2) &= \frac{1}{2}\big(\tilde{W}_2(k_1,k_2) - \tilde{W}_3(k_1,k_2)\big)\,, \\
\tilde{W}_{++}(k_1,k_2) &= \tilde{W}_4(k_1,k_2)\,.
\end{aligned} \tag{59}
$$

We show how the two-variate functions $\tilde{W}_j$ may be determined if $S^{(ab)}$ is known. The idea is to solve (56) perturbatively and compare the result with Equation (55). The first-order solution of (56) coincides with the spatial Fourier transform of Equation (39),

$$
\tilde{\zeta}^{[1]}(k) = \sum_a F^{(a)}\ \exp(-i\Omega^{(a)}(k)t)\,, \tag{60}
$$

where

$$
F^{(a)} = -C^{(a)}\frac{k}{\Omega^{(a)}}\left(A^{(a)}\cosh kh - A^{(a)}\cosh\kappa^{(a)}h + B^{(a)}\sinh\kappa^{(a)}h - \frac{\kappa^{(a)}}{k}B^{(a)}\sinh kh\right) \tag{61}
$$

Certainly, the expression of the coefficients is arbitrary, so the specific form (61) may be chosen without restricting generality. It is suitable for making contact with the previous calculations.

The second-order solution satisfies

$$\begin{aligned}
&\frac{\partial^2 \tilde{\zeta}^{[2]}(k)}{\partial t^2} + i\Big[\Omega^{(1)}(k) + \Omega^{(2)}(k)\Big]\frac{\partial \tilde{\zeta}^{[2]}(k)}{\partial t} - \Omega^{(1)}(k)\Omega^{(2)}(k)\tilde{\zeta}^{[2]}(k) \\
&+ \int_{-\infty}^{\infty} dk'\ \tilde{W}_1(k', k-k')\tilde{\zeta}^{[1]}(k')\tilde{\zeta}^{[1]}(k-k') \\
&+\frac{1}{2}\int_{-\infty}^{\infty} dk'\ \tilde{W}_2(k', k-k')\left(\tilde{\zeta}^{[1]}(k')\frac{\partial \tilde{\zeta}^{[1]}(k-k')}{\partial t} + \frac{\partial \tilde{\zeta}^{[1]}(k')}{\partial t}\tilde{\zeta}^{[1]}(k-k')\right) \\
&+\frac{1}{2}\int_{-\infty}^{\infty} dk'\ \tilde{W}_3(k', k-k')\left(\tilde{\zeta}^{[1]}(k')\frac{\partial \tilde{\zeta}^{[1]}(k-k')}{\partial t} - \frac{\partial \tilde{\zeta}^{[1]}(k')}{\partial t}\tilde{\zeta}^{[1]}(k-k')\right) \\
&+ \int_{-\infty}^{\infty} dk'\ \tilde{W}_4(k', k-k')\frac{\partial \tilde{\zeta}^{[1]}(k')}{\partial t}\frac{\partial \tilde{\zeta}^{[1]}(k-k')}{\partial t} = 0\,.
\end{aligned} \tag{62}$$

The homogeneous part of the solution may be included in the first-order solution; hence, it suffices to construct the particular solution with the same time dependence as the correction term, i.e.,

$$\tilde{\zeta}^{[2]}(k) = \sum_a \sum_b \int_{\infty}^{\infty} dk'\ C^{(a)}(k')C^{(b)}(k-k')\hat{S}^{(ab)}(k', k-k')\ \exp\Big(-i\Big[\Omega^{(a)}(k') + \Omega^{(b)}(k-k')\Big]t\Big) \tag{63}$$

which is identical with Equation (55). Upon inserting Equations (60) and (63) into Equation (62), we have

$$\tilde{W}_{--} - i\Omega^{(a)}(k')\tilde{W}_{+-} - i\Omega^{(b)}(k-k')\tilde{W}_{-+} - \Omega^{(a)}(k')\Omega^{(b)}(k-k')\tilde{W}_{++} = R^{(ab)}(k', k-k') \tag{64}$$

where

$$\begin{aligned}
&R^{(ab)}(k', k-k') = -\frac{C^{(a)}(k')C^{(b)}(k-k')}{F^{(a)}(k')F^{(b)}(k-k')}\hat{S}^{(ab)}(k', k-k') \\
&\times\Big\{-\Big[\Omega^{(a)}(k') + \Omega^{(b)}(k-k')\Big]^2 + \Big[\Omega^{(1)}(k) + \Omega^{(2)}(k)\Big]\Big[\Omega^{(a)}(k') + \Omega^{(b)}(k-k')\Big] \\
&-\Omega^{(1)}(k)\Omega^{(2)}(k)\Big\}
\end{aligned} \tag{65}$$

Note that $R^{(ab)}$ is independent of $C^{(a)}$ and $C^{(b)}$, due to (61). Since branch indices a and b can be both either 1 or 2, the set of equations (64) can be solved for any given k and k' values:

$$\begin{aligned}
\tilde{W}_{--} &= \frac{\Omega^{(2)}(k')\Omega^{(2)}(k-k')R^{(11)} + \Omega^{(1)}(k')\Omega^{(1)}(k-k')R^{(22)}}{[\Omega^{(1)}(k') - \Omega^{(2)}(k')]\,[\Omega^{(1)}(k-k') - \Omega^{(2)}(k-k')]} \\
&\quad - \frac{\Omega^{(2)}(k')\Omega^{(1)}(k-k')R^{(12)} + \Omega^{(1)}(k')\Omega^{(2)}(k-k')R^{(21)}}{[\Omega^{(1)}(k') - \Omega^{(2)}(k')]\,[\Omega^{(1)}(k-k') - \Omega^{(2)}(k-k')]} \\
\tilde{W}_{-+} &= i\frac{\Omega^{(1)}(k')\Big(R^{(21)} - R^{(22)}\Big) + \Omega^{(2)}(k')\Big(R^{(12)} - R^{(11)}\Big)}{[\Omega^{(1)}(k') - \Omega^{(2)}(k')]\,[\Omega^{(1)}(k-k') - \Omega^{(2)}(k-k')]} \\
\tilde{W}_{+-} &= i\frac{\Omega^{(1)}(k-k')\Big(R^{(212)} - R^{(22)}\Big) + \Omega^{(2)}(k-k')\Big(R^{(21)} - R^{(11)}\Big)}{[\Omega^{(1)}(k') - \Omega^{(2)}(k')]\,[\Omega^{(1)}(k-k') - \Omega^{(2)}(k-k')]} \\
\tilde{W}_{++} &= \frac{R^{(12)} + R^{(21)} - R^{(11)} - R^{(22)}}{[\Omega^{(1)}(k') - \Omega^{(2)}(k')]\,[\Omega^{(1)}(k-k') - \Omega^{(2)}(k-k')]}\,.
\end{aligned} \tag{66}$$

With this, Equation (58) is completely defined.

6. Numerical Results

As reference, computational modelling was utilized to simulate the physical problem under consideration. The computational simulations were executed via the open-source computational fluid dynamics (CFD) software, OpenFOAM. This platform offered an efficient and highly versatile framework for testing the varied parameters that impact the problem. The geometry is a two-dimensional rectangular configuration, as shown in Figure 4. Our simulations accounted for several depths that corresponded to both propagation and non-propagation modes for glycerine in the presence of viscosity and surface tension, enabling a comprehensive understanding of the surface-wave propagation. In addition, we considered both linear and nonlinear regimes, thus broadening our approach to investigate the first- and the second-order solutions.

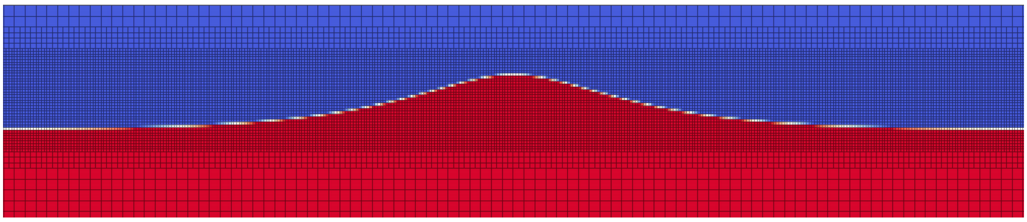

Figure 4. The initial wave shape. The defining wave parameters and fluid parameters are water depth: $d = 0.11$ mm; wave height: $h = 5$ mm; viscosity: $\nu = 0.0011197\ \frac{\text{Kg}}{\text{m.s}}$; density: $\rho = 1261$ (kg/m³); surface tension: $\sigma = 0.0635$ (N/m).

The chosen solver for our simulations was inteFoam, recognized for its suitability in handling free-surface flow problems. The computational domain was a box of dimensions one cubic meter. This size was deemed appropriate for capturing the key phenomena without imposing prohibitive computational demands. The initial wave profile used in our simulations was a Gaussian wave packet, selected for its ability to represent a localized disturbance while maintaining a continuous and differentiable waveform.

In the linear regime, we set the wave amplitude to 1/50 of the depth. As illustrated in Figure 5, this configuration confirmed the linear behaviour as discussed in [33]. On the other hand, for the nonlinear regime, the wave amplitude was set to half the depth. This resulted in the formation of a double hump, a characteristic feature corresponding to the second-order approximation. The observation of this feature provided an affirmation of the nonlinear dynamics inherent in our theoretical approach and simulation model. Hence, through the use of OpenFOAM and the specific simulation parameters, our study supports the second-order perturbative-approach theory, providing a comprehensive understanding of the capillary–gravity surface wave propagation.

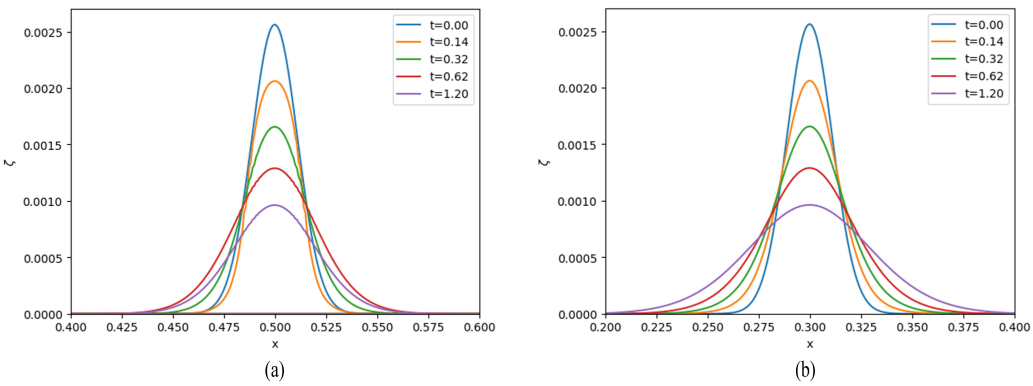

Figure 5. Comparing theoretical (**b**) and direct simulation (**a**) results.

7. Conclusions

This work presents a novel tool, the surface-wave equation, Equation (58), developed specifically for investigating the complex interplay between nonlinearity, dispersion and dissipation. While this equation is exact in the absence of nonlinear terms, the novelty lies in the inclusion of these nonlinear terms, underscoring the importance of nonlinearity in the overall framework.

Second-order perturbation theory of the Navier–Stokes equations for free-surface flows was presented, with wave amplitude considered as the perturbation parameter. The results allowed a systematic derivation of a nonlinear-surface-wave equation. To this end, the most general quadratic second-order differential equation permissible under horizontal translational symmetry was formulated. It contains four unknown functions. Then, perturbation theory up to the second order is applied to this equation. This solution is compared with that of the previous perturbation theory applied to Navier–Stokes equations. This comparison allows for the determination of the four previously unknown functions.

No assumptions concerning the wavelength-to-layer-width ratio were made. Hence, the equation takes into account linear dispersion fully, while nonlinearity is included in leading order.

It should be noted that while the concept presented here can be extended to higher orders, one limitation is that we have neglected the presence of the infinitely many over-damped modes and kept only the two least-damped ones. Due to nonlinear coupling among the modes, this means that our equation may lead initially, when nonlinearity is significant, to somewhat slower decay than in reality. The extent of this should be still estimated.

The results contain rather long expressions that are difficult to handle. Therefore, discussion of special cases—like weakly damped waves—requires further efforts and is beyond the scope of the present paper. A further important open question is how our equation can be solved in a numerically effective way. Note that nonlinear dispersion relations remain outside the scope of this investigation as the surface-wave equation lacks an analytical solution.

Surface waves exhibit inherent nonlinearity, which can activate dormant linear modes and lead to enhanced attenuation if the secondary modes are over-damped. Conversely, if the primary modes are over-damped and the secondary modes are under-damped, nonlinearity may propagate their appearance. These effects are not expected within a linear approximation, highlighting the significance of considering nonlinearity when analyzing surface-wave behavior. Nonlinearity in wave equations can cause a variety of complex phenomena, including frequency modulation, wave mixing and mode formation, solitons, breeders, nonlinear resonances and modulational instabilities. These events are expected to remain in some form even when dissipation is present.

With regards to applications, the most intriguing circumstances involve strong nonlinearity coupled with weak dissipation. Despite this, this study investigates situations with weak nonlinearity and arbitrary dissipation, primarily excited by intellectual curiosity and a desire to define solitons amidst dissipation. This parameter setting can have direct application when examining highly viscous fluids such as oil and even in the studies involving freezing thick fluids [45].

Author Contributions: Methodology, A.G. and G.B.; Validation, G.B.; Formal analysis, A.G. and G.B.; Investigation, A.G. and G.B.; Writing—original draft, A.G.; Writing—review & editing, A.G. and G.B.; Supervision, G.B. All authors have read and agreed to the published version of the manuscript.

Funding: This research received no external funding.

Acknowledgments: This research was supported by the Ministry of Culture and Innovation and the National Research. A.G. greatly acknowledges the support from Stipendium Hungaricum No. 228712. We are indebted to our reviewers for their many helpful comments and suggestions.

Conflicts of Interest: The authors declare no conflict of interest.

Appendix A

Coefficients in Equation (46):

$$
\begin{aligned}
\bar{\alpha}_{c+}^{(ab)} &= 0 \\
\bar{\beta}_{c+}^{(ab)} &= \frac{i}{4}\left(k_1-\kappa_1^{(a)}\right)\left(k_1^2-\kappa_1^{(a)2}\right)\left(k_2A_2^{(b)}B_1^{(a)}+\kappa_2^{(b)}A_1^{(a)}B_2^{(b)}\right) \\
\bar{\gamma}_{c+}^{(ab)} &= \frac{i}{4}\left(k_2-\kappa_2^{(b)}\right)\left(k_2^2-\kappa_2^{(b)2}\right)\left(k_1A_1^{(a)}B_2^{(b)}+\kappa_1^{(a)}A_2^{(b)}B_1^{(a)}\right) \\
\bar{\delta}_{c+}^{(ab)} &= -\frac{i}{4}\left(k_2^2-k_1^2+\kappa_1^{(a)2}-\kappa_2^{(b)2}\right)\left(\kappa_1^{(a)}k_2-\kappa_2^{(b)}k_1\right)\left(A_1^{(a)}B_2^{(b)}+A_2^{(b)}B_1^{(a)}\right) \\
\bar{\alpha}_{c-}^{(ab)} &= 0 \\
\bar{\beta}_{c-}^{(ab)} &= -\frac{i}{4}\left(k_1+\kappa_1^{(a)}\right)\left(k_1^2-\kappa_1^{(a)2}\right)\left(k_2A_2^{(b)}B_1^{(a)}-\kappa_2^{(b)}A_1^{(a)}B_2^{(b)}\right) \\
\bar{\gamma}_{c-}^{(ab)} &= -\frac{i}{4}\left(k_2+\kappa_2^{(b)}\right)\left(k_2^2-\kappa_2^{(b)2}\right)\left(k_1A_1^{(a)}B_2^{(b)}-\kappa_1^{(a)}A_2^{(b)}B_1^{(a)}\right) \\
\bar{\delta}_{c-}^{(ab)} &= \frac{i}{4}\left(k_2^2-k_1^2+\kappa_1^{(a)2}-\kappa_2^{(b)2}\right)\left(\kappa_1^{(a)}k_2+\kappa_2^{(b)}k_1\right)\left(A_1^{(a)}B_2^{(b)}-A_2^{(b)}B_1^{(a)}\right) \\
\bar{\alpha}_{s+}^{(ab)} &= 0 \\
\bar{\beta}_{s+}^{(ab)} &= -\frac{i}{4}\left(k_1-\kappa_1^{(a)}\right)\left(k_1^2-\kappa_1^{(a)2}\right)\left(k_2A_1^{(a)}A_2^{(b)}+\kappa_2^{(b)}B_1^{(a)}B_2^{(b)}\right) \\
\bar{\gamma}_{s+}^{(ab)} &= -\frac{i}{4}\left(k_2-\kappa_2^{(b)}\right)\left(k_2^2-\kappa_2^{(b)2}\right)\left(k_1A_1^{(a)}A_2^{(b)}+\kappa_1^{(a)}B_1^{(a)}B_2^{(b)}\right) \\
\bar{\delta}_{s+}^{(ab)} &= \frac{i}{4}\left(k_2^2-k_1^2+\kappa_1^{(a)2}-\kappa_2^{(b)2}\right)\left(\kappa_1^{(a)}k_2-\kappa_2^{(b)}k_1\right)\left(A_1^{(a)}A_2^{(b)}+B_1^{(a)}B_2^{(b)}\right) \\
\bar{\alpha}_{s-}^{(ab)} &= 0 \\
\bar{\beta}_{s-}^{(ab)} &= \frac{i}{4}\left(k_1+\kappa_1^{(a)}\right)\left(k_1^2-\kappa_1^{(a)2}\right)\left(k_2A_1^{(a)}A_2^{(b)}-\kappa_2^{(b)}A_1^{(a)}A_2^{(b)}\right) \\
\bar{\gamma}_{s-}^{(ab)} &= -\frac{i}{4}\left(k_2+\kappa_2^{(b)}\right)\left(k_2^2-\kappa_2^{(b)2}\right)\left(k_1A_1^{(a)}A_2^{(b)}-\kappa_1^{(a)}B_1^{(a)}B_2^{(b)}\right) \\
\bar{\delta}_{s-}^{(ab)} &= \frac{i}{4}\left(k_2^2-k_1^2+\kappa_1^{(a)2}-\kappa_2^{(b)2}\right)\left(\kappa_1^{(a)}k_2+\kappa_2^{(b)}k_1\right)\left(A_1^{(a)}A_2^{(b)}-B_1^{(a)}B_2^{(b)}\right)
\end{aligned} \tag{A1}
$$

Coefficients in Equation (47):

$$
\begin{aligned}
\alpha_{c+}^{(ab)} &= 0 \\
\beta_{c+}^{(ab)} &= \frac{i}{4\nu}\frac{\left(k_1^2-\kappa_1^{(a)2}\right)\left(k_2A_2^{(b)}B_1^{(a)}+\kappa_2^{(b)}A_1^{(a)}B_2^{(b)}\right)}{\left(k_1+2k_2+\kappa_1^{(a)}\right)\left(k_2^2-2k_1k_2+2\kappa_1^{(a)}k_2-\kappa_2^{(b)2}\right)} \\
\gamma_{c+}^{(ab)} &= \frac{i}{4\nu}\frac{\left(k_2^2-\kappa_2^{(b)2}\right)\left(k_1A_1^{(a)}B_2^{(b)}+\kappa_1^{(a)}A_2^{(b)}B_1^{(a)}\right)}{\left(k_2+2k_1+\kappa_2^{(b)}\right)\left(k_1^2-2k_1k_2+2\kappa_2^{(b)}k_1-\kappa_1^{(a)2}\right)} \\
\delta_{c+}^{(ab)} &= \frac{i}{8\nu}\frac{\left(k_2^2-k_1^2+\kappa_1^{(a)2}-\kappa_2^{(b)2}\right)\left(\kappa_1^{(a)}k_2-\kappa_2^{(b)}k_1\right)\left(A_1^{(a)}B_2^{(b)}+A_2^{(b)}B_1^{(a)}\right)}{\left[(k_1+k_2)^2-\left(\kappa_1^{(a)}+\kappa_2^{(b)}\right)^2\right]\left(k_1k_2-\kappa_1^{(a)}\kappa_2^{(b)}\right)} \\
\alpha_{c-}^{(ab)} &= 0 \\
\beta_{c-}^{(ab)} &= -\frac{i}{4\nu}\frac{\left(k_1^2-\kappa_1^{(a)2}\right)\left(k_2A_2^{(b)}B_1^{(a)}-\kappa_2^{(b)}A_1^{(a)}B_2^{(b)}\right)}{\left(k_1+2k_2-\kappa_1^{(a)}\right)\left(k_2^2-2k_1k_2-2\kappa_1^{(a)}k_2-\kappa_2^{(b)2}\right)} \\
\gamma_{c-}^{(ab)} &= -\frac{i}{4\nu}\frac{\left(k_2^2-\kappa_2^{(b)2}\right)\left(k_1A_1^{(a)}B_2^{(b)}-\kappa_1^{(a)}A_2^{(b)}B_1^{(a)}\right)}{\left(k_2+2k_1-\kappa_2^{(b)}\right)\left(k_1^2-2k_1k_2-2\kappa_2^{(b)}k_1-\kappa_1^{(a)2}\right)}
\end{aligned}
$$

$$
\begin{aligned}
\delta_{c-}^{(ab)} &= -\frac{i}{8\nu}\frac{\left(k_2^2-k_1^2+\kappa_1^{(a)2}-\kappa_2^{(b)2}\right)\left(\kappa_1^{(a)}k_2+\kappa_2^{(b)}k_1\right)\left(A_1^{(a)}B_2^{(b)}-A_2^{(b)}B_1^{(a)}\right)}{\left[(k_1+k_2)^2-\left(\kappa_1^{(a)}-\kappa_2^{(b)}\right)^2\right]\left(k_1k_2+\kappa_1^{(a)}\kappa_2^{(b)}\right)} \\
\alpha_{s+}^{(ab)} &= 0 \\
\beta_{s+}^{(ab)} &= -\frac{i}{4\nu}\frac{\left(k_1^2-\kappa_1^{(a)2}\right)\left(k_2A_1^{(a)}A_2^{(b)}+\kappa_2^{(b)}B_1^{(a)}B_2^{(b)}\right)}{\left(k_1+2k_2+\kappa_1^{(a)}\right)\left(k_2^2-2k_1k_2+2\kappa_1^{(a)}k_2-\kappa_2^{(b)2}\right)} \\
\gamma_{s+}^{(ab)} &= -\frac{i}{4\nu}\frac{\left(k_2^2-\kappa_2^{(b)2}\right)\left(k_1A_1^{(a)}A_2^{(b)}+\kappa_1^{(a)}B_1^{(a)}B_2^{(b)}\right)}{\left(k_2+2k_1+\kappa_2^{(b)}\right)\left(k_1^2-2k_1k_2+2\kappa_2^{(b)}k_1-\kappa_1^{(a)2}\right)} \\
\delta_{s+}^{(ab)} &= -\frac{i}{8\nu}\frac{\left(k_2^2-k_1^2+\kappa_1^{(a)2}-\kappa_2^{(b)2}\right)\left(\kappa_1^{(a)}k_2-\kappa_2^{(b)}k_1\right)\left(A_1^{(a)}A_2^{(b)}+B_1^{(a)}B_2^{(b)}\right)}{\left[(k_1+k_2)^2-\left(\kappa_1^{(a)}+\kappa_2^{(b)}\right)^2\right]\left(k_1k_2-\kappa_1^{(a)}\kappa_2^{(b)}\right)} \\
\alpha_{s-}^{(ab)} &= 0 \\
\beta_{s-}^{(ab)} &= \frac{i}{4\nu}\frac{\left(k_1^2-\kappa_1^{(a)2}\right)\left(k_2A_1^{(a)}A_2^{(b)}-\kappa_2^{(b)}A_1^{(a)}A_2^{(b)}\right)}{\left(k_1+2k_2-\kappa_1^{(a)}\right)\left(k_2^2-2k_1k_2-2\kappa_1^{(a)}k_2-\kappa_2^{(b)2}\right)} \\
\gamma_{s-}^{(ab)} &= -\frac{i}{4\nu}\frac{\left(k_2^2-\kappa_2^{(b)2}\right)\left(k_1A_1^{(a)}A_2^{(b)}-\kappa_1^{(a)}B_1^{(a)}B_2^{(b)}\right)}{\left(k_2+2k_1-\kappa_2^{(b)}\right)\left(k_1^2-2k_1k_2-2\kappa_2^{(b)}k_1-\kappa_1^{(a)2}\right)} \\
\delta_{s-}^{(ab)} &= -\frac{i}{8\nu}\frac{\left(k_2^2-k_1^2+\kappa_1^{(a)2}-\kappa_2^{(b)2}\right)\left(\kappa_1^{(a)}k_2+\kappa_2^{(b)}k_1\right)\left(A_1^{(a)}A_2^{(b)}-B_1^{(a)}B_2^{(b)}\right)}{\left[(k_1+k_2)^2-\left(\kappa_1^{(a)}-\kappa_2^{(b)}\right)^2\right]\left(k_1k_2+\kappa_1^{(a)}\kappa_2^{(b)}\right)}
\end{aligned}
\tag{A2}
$$

References

1. Matsuno, Y. Nonlinear evolutions of surface gravity waves on fluid of finite depth. *Phys. Rev. Lett.* **1992**, *69*, 609. [CrossRef] [PubMed]
2. Artiles, W.; Nachbin, A. Nonlinear evolution of surface gravity waves over highly variable depth. *Phys. Rev. Lett.* **2004**, *93*, 234501. [CrossRef] [PubMed]
3. Wang, Z.; Milewski, P.A. Dynamics of gravity–capillary solitary waves in deep water. *J. Fluid Mech.* **2012**, *708*, 480–501. [CrossRef]
4. Belibassakis, K.; Touboul, J. A nonlinear coupled-mode model for waves propagating in vertically sheared currents in variable bathymetry—Collinear waves and currents. *Fluids* **2019**, *4*, 61. [CrossRef]
5. Gao, T.; Milewski, P.; Wang, Z. Capillary–gravity solitary waves on water of finite depth interacting with a linear shear current. *Stud. Appl. Math.* **2021**, *147*, 1036–1057. [CrossRef]
6. Li, Y. A Mathematical Model for Nonlinear Gravity–Capillary Waves in a Large Temporal-Spatial Domain. In Porceedings of the EGU General Assembly 2023, Vienna, Austria, 24–28 April 2023; EGU23-13972
7. Ambrose, D.; Bona, J.; Nicholls, D. Well-Posedness of a Model for Water Waves with Viscosity. *DIscrete Continous Dyn. Syst. Ser. B* **2012**, *17*, 4. [CrossRef]
8. Kurkina, O.; Kurkin, A.; Pelinovsky, E.; Stepanyants, Y.; Talipova, T. Nonlinear Models of Finite Amplitude Interfacial Waves in Shallow Two-Layer Fluid. In *Applied Wave Mathematics II: Selected Topics in Solids, Fluids, and Mathematical Methods and Complexity*; Springer: Cham, Switzerland, 2019; pp. 61–87.
9. Liu, J.; Hayatdavoodi, M.; Ertekin, R.C. A Comparative Study on Generation and Propagation of Nonlinear Waves in Shallow Waters. *J. Mar. Sci. Eng.* **2023**, *11*, 917. [CrossRef]
10. Giamagas, G.; Zonta, F.; Roccon, A.; Soldati, A. Propagation of capillary waves in two-layer oil–water turbulent flow. *J. Fluid Mech.* **2023**, *960*, A5. [CrossRef]
11. Mao, Y.; Hoefer, M.A. Experimental investigations of linear and nonlinear periodic travelling waves in a viscous fluid conduit. *J. Fluid Mech.* **2023**, *954*, A14. [CrossRef]

12. Clamond, D.; Dutykh, D. Accurate fast computation of steady two-dimensional surface gravity waves in arbitrary depth. *J. Fluid Mech.* **2018**, *844*, 491–518. [CrossRef]
13. Khatskevich, V.L. On the asymptotics of the motion of a nonlinear viscous fluid. *Sib. Math. J.* **2017**, *58*, 329–337. [CrossRef]
14. Jiang, S.C.; Liu, C.F.; Sun, L. Numerical comparison for focused wave propagation between the fully nonlinear potential flow and the viscous fluid flow models. *China Ocean. Eng.* **2020**, *34*, 279–288. [CrossRef]
15. Harrison, W. The influence of viscosity and capillarity on waves of finite amplitude. *Proc. Lond. Math. Soc.* **1909**, *2*, 107–121. [CrossRef]
16. Dias, F.; Kharif, C. Nonlinear gravity and capillary–gravity waves. *Annu. Rev. Fluid Mech.* **1999**, *31*, 301–346. [CrossRef]
17. Hunt, J.N. Interfacial waves of finite amplitude. *La Houille Blanche* **1961** , *4*, 515–531. [CrossRef]
18. Tsuji, Y.; Nagata, Y. Stokes' expansion of internal deep water waves to the fifth order. *J. Oceanogr. Soc. Jpn.* **1973**, *29*, 61–69.
19. Trulsen, K.; Kliakhandler, I.; Dysthe, K.B.; Velarde, M.G. On weakly nonlinear modulation of waves on deep water. *Phys. Fluids* **2000**, *12*, 2432–2437. [CrossRef]
20. Stiassnie, M. Note on the modified nonlinear Schrödinger equation for deep water waves. *Wave Motion* **1984**, *6*, 431–433. [CrossRef]
21. Sulem, C.; Sulem, P.L. *The Nonlinear SchröDinger Equation: Self-Focusing and Wave Collapse*; Springer Science & Business Media: New York, NY, USA, 2007; Volume 139.
22. Dysthe, K.B. Note on a modification to the nonlinear Schrödinger equation for application to deep water waves. *Proc. R. Soc. Lond. Math. Phys. Sci.* **1979**, *369*, 105–114.
23. Lamb, H. *Hydrodynamics*; Dover Publications: New York, NY, USA, 1945; p. 445.
24. Landau, L.D.; Lifshitz, E.M. *Fluid Mechanics: Landau and Lifshitz: Course of Theoretical Physics*; Elsevier: Amsterdam, The Netherlands, 2013; Volume 6.
25. Robertson, S.; Rousseaux, G. Viscous dissipation of surface waves and its relevance to analogue gravity experiments. *arXiv* **2017**, arXiv:1706.05255.
26. Dias, F.; Dyachenko, A.I.; Zakharov, V.E. Theory of weakly damped free-surface flows: A new formulation based on potential flow solutions. *Phys. Lett.* **2008**, *372*, 1297–1302. [CrossRef]
27. Liu, C.M.; Hwung, H.H.; Yang, R.Y. On the study of second-order wave theory and its convergence for a two-fluid system. *Math. Probl. Eng.* **2013**, *2013*, 253401. [CrossRef]
28. Longuet-Higgins, M.S. Mass transport in water waves. *Philos. Trans. R. Soc. Lond. Ser. Math. Phys. Sci.* **1953**, *245*, 535–581.
29. Longuet-Higgins, M. Mass transport in the boundary layer at a free oscillating surface. *J. Fluid Mech.* **1960**, *8*, 293–306. [CrossRef]
30. Debnath, L.; Basu, K. Nonlinear water waves and nonlinear evolution equations with applications. In *Solitons*; Springer: New York, NY, USA, 2022; p. 1.
31. Vitanov, N.K.; Ivanova, T.I. Solitary wave solutions of several nonlinear PDEs modeling shallow water waves. *arXiv* **2017**, arXiv:1709.05320.
32. Barannyk, L.L.; Papageorgiou, D.T. Fully nonlinear gravity–capillary solitary waves in a two-fluid system of finite depth. *J. Eng. Math.* **2002**, *42*, 321–339. [CrossRef]
33. Ghahraman, A.; Bene, G. Bifurcation Analysis and Propagation Conditions of Free-Surface Waves in Incompressible Viscous Fluids of Finite Depth. *Fluids* **2023**, *8*, 173. [CrossRef]
34. Le Meur, H.V. Derivation of a viscous Boussinesq system for surface water waves. *Asymptot. Anal.* **2015**, *94*, 309–345. [CrossRef]
35. Armaroli, A.; Eeltink, D.; Brunetti, M.; Kasparian, J. Viscous damping of gravity–capillary waves: Dispersion relations and nonlinear corrections. *Phys. Rev. Fluids* **2018**, *3*, 124803. [CrossRef]
36. Ammar, N.; Ali, H.A. Mathematical Modelling for Peristaltic Flow of Sutterby Fluid Through Tube under the Effect of Endoscope. *Iraqi J. Sci.* **2023**, 2368–2381. [CrossRef]
37. Nazeer, M.; Alqarni, M.Z.; Hussain, F.; Saleem, S. Computational analysis of multiphase flow of non-Newtonian fluid through inclined channel: Heat transfer analysis with perturbation method. *Comput. Part. Mech.* **2023**, *10*, 1371–1381.
38. Rafiq, M.; Abbas, Z.; Hasnain, J. Theoretical exploration of thermal transportation with Lorentz force for fourth-grade fluid model obeying peristaltic mechanism. *Arab. J. Sci. Eng.* **2021**, *46*, 12391–12404. [CrossRef]
39. Abbas, Z.; Rafiq, M.; Hasnain, J.; Umer, H. Impacts of lorentz force and chemical reaction on peristaltic transport of Jeffrey fluid in a penetrable channel with injection/suction at walls. *Alex. Eng. J.* **2021**, *60*, 1113–1122. [CrossRef]
40. Abbas, Z.; Rafiq, M.; Hasnain, J.; Javed, T. Peristaltic transport of a Casson fluid in a non-uniform inclined tube with Rosseland approximation and wall properties. *Arab. J. Sci. Eng.* **2021**, *46*, 1997–2007. [CrossRef]
41. Jian, Y.; Zhu, Q.; Zhang, J.; Wang, Y. Third order approximation to capillary gravity short crested waves with uniform currents. *Appl. Math. Model.* **2009**, *33*, 2035–2053. [CrossRef]
42. Farsoiya, P.K.; Mayya, Y.; Dasgupta, R. Axisymmetric viscous interfacial oscillations–theory and simulations. *J. Fluid Mech.* **2017**, *826*, 797–818. [CrossRef]
43. Boujelbene, M.; Hadimani, B.; Choudhari, R.; Sanil, P.; Gudekote, M.; Vaidya, H.; Prasad, K.V.; Fadhl, B.M.; Makhdoum, B.M.; Ijaz Khan, M.; et al. Impact of Variable Slip and Wall Properties on Peristaltic Flow of Eyring—Powell Fluid Through Inclined Channel: Artificial Intelligence Based Perturbation Technique. *Fractals* **2023**, *31*, 2340140. [CrossRef]

44. Hunt, J.N. The viscous damping of gravity waves in shallow water. *La Houille Blanche* **1964**, *6*, 685–691. [CrossRef]
45. Dubrovin, B. *Dispersion Relations for Nonlinear Waves and the Schottky Problem*; Springer: Berlin/Heidelberg, Germany, 2012; pp. 86–98.